



UNIVERSITY OF LEEDS

This is a repository copy of *A weakly overlapping domain decomposition preconditioner for the finite element solution of elliptic partial differential equations*.

White Rose Research Online URL for this paper:
<http://eprints.whiterose.ac.uk/1736/>

Article:

Bank, R.E., Jimack, P.K., Nadeem, S.A. et al. (1 more author) (2002) A weakly overlapping domain decomposition preconditioner for the finite element solution of elliptic partial differential equations. *SIAM Journal on Scientific Computing*, 23 (6). pp. 1817-1841. ISSN 1064-8275

<https://doi.org/10.1137/S1064827501361425>

Reuse

See Attached

Takedown

If you consider content in White Rose Research Online to be in breach of UK law, please notify us by emailing eprints@whiterose.ac.uk including the URL of the record and the reason for the withdrawal request.



eprints@whiterose.ac.uk
<https://eprints.whiterose.ac.uk/>



White Rose
university consortium
Universities of Leeds, Sheffield & York

White Rose Consortium ePrints Repository

<http://eprints.whiterose.ac.uk/>

This is an author produced version of a paper published in **SIAM Journal on Scientific Computing**.

White Rose Repository URL for this paper:

<http://eprints.whiterose.ac.uk/1736/>

Published paper

Bank, R.E., Jimack, P.K., Nadeem, S.A. and Nepomnyaschikh, S.V. (2002) *A weakly overlapping domain decomposition preconditioner for the finite element solution of elliptic partial differential equations*. SIAM Journal on Scientific Computing, 23 (6). pp. 1817-1841.

A Weakly Overlapping Domain Decomposition Preconditioner for the Finite Element Solution of Elliptic Partial Differential Equations

R.E. Bank*, P.K. Jimack†, S.A. Nadeem† and S.V. Nepomnyaschikh‡

Abstract

We present a new two level additive Schwarz domain decomposition preconditioner which is appropriate for use in the parallel finite element solution of elliptic partial differential equations (PDEs). As with most parallel domain decomposition methods each processor may be assigned one or more subdomains and the preconditioner is such that the processors are able to solve their own subproblem(s) concurrently. The novel feature of the technique proposed here is that it requires just a single layer of overlap in the elements which make up each subdomain at each level of refinement, and it is shown that this amount of overlap is sufficient to yield an optimal preconditioner. Some numerical experiments are included to confirm that the condition number when using the new preconditioner is indeed independent of the level of mesh refinement on the test problems considered: which are posed in both two and three space dimensions.

1 Introduction

In this paper we introduce a two level overlapping additive Schwarz (AS) algorithm which may be applied as an optimal domain decomposition (DD) preconditioner for the adaptive finite element solution of a variety of second-order self-adjoint elliptic problems defined on a bounded Lipschitz domain $\Omega \subset \mathbb{R}^n$ ($n = 2, 3$). In recent years there has been a large amount of research into DD and related methods and we refer to some of the recent survey and review articles, such as [11, 24, 27, 30, 36, 37], for further details. In particular we note that a number of the algorithms proposed have been successfully implemented as software (see, for example, [12, 16, 21]) and many take the form of multiplicative or multilevel methods (e.g. [3, 8, 10, 15, 38]). Furthermore, by viewing these iterative techniques in terms of subspace corrections it is possible to develop a unified theory for a variety of algorithms and so, although this paper mainly discusses a two level additive Schwarz approach, it is certainly possible to generalize this to a multiplicative or a multilevel variant. This is briefly considered in Section 6.

Although the work in this paper applies in both two and three dimensions, the first four sections consider the following model problem in just two dimensions so as to simplify the explanations and illustrations provided. In Section 5 the ideas presented are then generalized to three dimensions. It should also be noted that the ideas presented may also be applied to a wider variety of boundary conditions than the zero Dirichlet conditions imposed here for simplicity.

Problem 1.1 Find $u \in \mathcal{H}_0^1(\Omega)$ such that

$$\mathcal{A}(u, v) = \mathcal{F}(v) \quad \forall v \in \mathcal{H}_0^1(\Omega), \quad (1.1)$$

*Dept. of Mathematics, University of California at San Diego, La Jolla, CA 92093, USA.

†School of Computing, University of Leeds, Leeds LS2 9JT, UK.

‡Computing Centre, Siberian Branch of the Russian Academy of Sciences, Novosibirsk 630090, Russia.

where $\Omega \subset \mathbb{R}^2$ is the problem domain and

$$\mathcal{H}_0^1(\Omega) = \{u \in \mathcal{H}^1(\Omega) : u|_{\partial\Omega_E} = 0\} . \quad (1.2)$$

Here $\partial\Omega_E$ is a closed, non-empty subset of the boundary, $\partial\Omega$, upon which zero Dirichlet boundary conditions are imposed and $\mathcal{A}(\cdot, \cdot)$ and $\mathcal{F}(\cdot)$ are the bilinear and linear forms

$$\mathcal{A}(u, v) = \int_{\Omega} (P(\underline{x})\underline{\nabla}u) \cdot \underline{\nabla}v \, d\underline{x} \quad \text{and} \quad \mathcal{F}(v) = \int_{\Omega} f v \, d\underline{x} + \int_{\partial\Omega_N} g v \, ds , \quad (1.3)$$

where $P(\underline{x})$ is bounded, symmetric and strictly positive-definite, and $\partial\Omega_N = \partial\Omega - \partial\Omega_E$ is the part of the boundary subject to Neumann boundary conditions: $\underline{n} \cdot (P(\underline{x})\underline{\nabla}u) = g(\underline{x})$.

The Galerkin finite element (FE) method for the solution of (1.1) requires a triangulation, \mathcal{T}^h say, of Ω to be produced so that one may define a piecewise polynomial space of trial functions, \mathcal{V}^h say, on \mathcal{T}^h . Further details of the construction of this triangulation are given in the following sections and, for the sake of clarity, we only consider continuous piecewise linear finite element spaces on \mathcal{T}^h throughout the rest of this paper. Section 2 also provides background on the relevant theoretical and practical details of additive Schwarz preconditioning that are required for Section 3. This section introduces details of the DD preconditioner that we propose and presents a detailed analysis of its convergence properties. In the analysis it is demonstrated that it is possible to obtain an optimal preconditioner (i.e. with condition number independent of the mesh size and the number and size of the subdomains) with an overlap of just one element at each level of a mesh hierarchy. This is the main result of the paper. Finally, Sections 4 and 5 present a small number of numerical examples using the proposed DD preconditioner for two and three dimensional problems respectively. The paper concludes with a brief discussion of possible extensions and applications of this work.

2 Background

In order to approximate the solution of (1.1) from the finite dimensional space \mathcal{V}^h (of continuous piecewise linears on \mathcal{T}^h (where h is the diameter of the largest triangle)), it is necessary to solve the following discrete problem.

Problem 2.1 Find $u^h \in \mathcal{V}^h \cap \mathcal{H}_0^1(\Omega)$ such that

$$\mathcal{A}(u^h, v^h) = \mathcal{F}(v^h) \quad \forall v^h \in \mathcal{V}^h \cap \mathcal{H}_0^1(\Omega) . \quad (2.1)$$

This is achieved by choosing a basis for \mathcal{V}^h and expressing the problem as a matrix equation

$$A\underline{u} = \underline{b} . \quad (2.2)$$

For the usual, local, choice of basis the stiffness matrix A is sparse, symmetric and strictly positive-definite and so an iterative solution method, such as the conjugate gradient (CG) algorithm (e.g. [2, 17]), is most appropriate. However, it is well-known that, when the triangulation \mathcal{T}^h is uniformly refined, the condition number of A grows like $O(h^{-2})$ as $h \rightarrow 0$ (see [23] for example), hence it is necessary to apply a preconditioned version of the CG algorithm for realistic mesh sizes h .

In this work we consider the use of additive Schwarz preconditioning (e.g. [13, 14, 18, 25, 28, 33]), which is suitable for use with both non-uniformly refined meshes and parallel computer architectures.

Let us define $\mathcal{V} = \mathcal{V}^h \cap \mathcal{H}_0^1(\Omega)$ to be the trial and test space in (2.1) and assume that the triangulation \mathcal{T}^h may be obtained by the uniform refinement of some coarser triangulation, \mathcal{T}^H say, of the domain Ω , where \mathcal{V}_0 is the corresponding piecewise linear finite element space, $\mathcal{V}^H \cap \mathcal{H}_0^1(\Omega)$, defined on \mathcal{T}^H .

Having introduced a coarse mesh \mathcal{T}^H it is now possible to decompose Ω into (possibly overlapping) subdomains, $\Omega_1, \dots, \Omega_p$ say, which are each the union of triangles in \mathcal{T}^H . We now define the spaces $\mathcal{H}_0^1(\Omega_i) \subset \mathcal{L}^2(\Omega)$, for $i = 1, \dots, p$, to be the extensions of $\mathcal{H}^1(\Omega_i)$ for which

$$u(\underline{x}) = 0 \quad \forall \underline{x} \in (\Omega - \overline{\Omega_i}) \cup \partial\Omega_E, \quad (2.3)$$

and the corresponding finite dimensional spaces $\mathcal{V}_i = \mathcal{V}^h \cap \mathcal{H}_0^1(\Omega_i)$. Note that these local spaces, \mathcal{V}_i , form a decomposition of the finite element space \mathcal{V} :

$$\mathcal{V} = \sum_{i=1}^p \mathcal{V}_i. \quad (2.4)$$

Thus, for each $v \in \mathcal{V}$, there exists a (not necessarily unique) combination of $v_i \in \mathcal{V}_i$ ($i = 1, \dots, p$) such that $v = \sum_{i=1}^p v_i$.

Given any space decomposition of the form (2.4), the additive Schwarz algorithm defines a preconditioner, B , for A in (2.2) in the following manner. Let Q_i be the projection from \mathcal{V} to \mathcal{V}_i (for $i = 1, \dots, p$) given by

$$\int_{\Omega} (Q_i u) v_i \, d\underline{x} = \int_{\Omega} u v_i \, d\underline{x} \quad \forall u \in \mathcal{V}, v_i \in \mathcal{V}_i, \quad (2.5)$$

and define \mathcal{A}_i to be the restriction of \mathcal{A} to $\mathcal{V}_i \times \mathcal{V}_i$ given by:

$$\mathcal{A}_i(u_i, v_i) = \mathcal{A}(u_i, v_i), \quad \forall u_i, v_i \in \mathcal{V}_i. \quad (2.6)$$

Note that (given the usual finite element bases for \mathcal{V} and \mathcal{V}_i) Q_i may be expressed as a rectangular matrix, \overline{Q}_i say, and a local stiffness matrix, A_i say, may be derived from \mathcal{A}_i (in the same way that the global stiffness matrix A is derived from \mathcal{A} above). The additive Schwarz (parallel subspace correction) preconditioner for (2.2) is then given by

$$B = \sum_{i=1}^p \overline{Q}_i^T A_i^{-1} \overline{Q}_i. \quad (2.7)$$

Note that each of the subdomain solves ($A_i^{-1} \underline{r}_i$), required when solving the system $B^{-1} \underline{s} = \underline{r}$ at each preconditioned CG iteration, may be performed concurrently and, for simplicity, we will assume for the time-being that all such subdomain solves are exact.

The following theorem, which is proved in [36] for example (or see [30] for a slightly more general form), provides the main theoretical justification for considering preconditioners of the form (2.7).

Theorem 2.1 *The matrix B defined by (2.7) is symmetric and positive-definite. Furthermore, if we assume that there is some constant $C > 0$ such that: for all $v \in \mathcal{V}$ there are $v_i \in \mathcal{V}_i$ such that $v = \sum_{i=1}^p v_i$ and*

$$\sum_{i=1}^p \mathcal{A}_i(v_i, v_i) \leq C \mathcal{A}(v, v), \quad (2.8)$$

then the spectral condition number of BA is given by

$$\kappa(BA) \leq \nu_c C, \quad (2.9)$$

where ν_c is the minimum number of colours required to colour the subdomains Ω_i in such a way that no neighbours are the same colour.

This result demonstrates that the quality of any AS preconditioner depends only upon the stability of the splitting of \mathcal{V} into subspaces \mathcal{V}_i . In particular, if the splitting is such that (2.8) holds with C independent of h , H or p then the preconditioner is said to be optimal.

Unfortunately, the decomposition described in equations (2.3) to (2.4) does not permit such a choice of C since it is entirely local in nature and so significant reductions in the low frequency error components can require many preconditioned CG iterations. This is easily rectified however by the introduction of an extra, coarse grid, term in the preconditioner (2.7):

$$B = \sum_{i=0}^p \overline{Q}_i^T A_i^{-1} \overline{Q}_i . \quad (2.10)$$

Here \overline{Q}_0 is another rectangular matrix corresponding to the \mathcal{L}^2 projection, Q_0 say, from \mathcal{V} to the coarse grid space \mathcal{V}_0 , given by,

$$\int_{\Omega} (Q_0 u) v_0 \, d\mathbf{x} = \int_{\Omega} u v_0 \, d\mathbf{x} \quad \forall u \in \mathcal{V}, v_0 \in \mathcal{V}_0 , \quad (2.11)$$

and A_0 is the stiffness matrix derived from \mathcal{A}_0 , the restriction of \mathcal{A} to $\mathcal{V}_0 \times \mathcal{V}_0$ given by

$$\mathcal{A}_0(u_0, v_0) = \mathcal{A}(u_0, v_0) \quad \forall u_0, v_0 \in \mathcal{V}_0 . \quad (2.12)$$

The following result is also proved in [30] and [36], and applies to the new two level preconditioner defined in (2.10).

Theorem 2.2 *Provided the overlap between the subdomains Ω_i is of size $O(H)$, where H represents the mesh size of \mathcal{T}^H , then there exists $C > 0$, which is independent of h , H and p , such that for any $v \in \mathcal{V}$ there are $v_i \in \mathcal{V}_i$ such that $v = \sum_{i=0}^p v_i$ and*

$$\sum_{i=0}^p \mathcal{A}_i(v_i, v_i) \leq C \mathcal{A}(v, v) . \quad (2.13)$$

The above result demonstrates that, provided a coarse-grid solve is undertaken and there is a “generous” overlap between the subdomains, the additive Schwarz technique may indeed be used to achieve optimal preconditioning. It should be noted however that these two provisos do raise important practical concerns over the efficiency of such a preconditioner. For example, the solution of the coarse-grid problem is hard to achieve in parallel and so care must be taken when developing parallel software to ensure that this does not become a significant bottleneck. More importantly however, the fixed $O(H)$ overlap that is required between the subdomains means that as the mesh \mathcal{T}^h is refined (assuming uniform global refinement for simplicity), the number of elements of \mathcal{T}^h in the overlap regions is $O(h^{-2})$ as $h \rightarrow 0$. This represents a significant computational overhead when h becomes small.

In practice the usual way in which this second issue is addressed (see, for example, [30]) is to drop the optimality requirement and only allow subdomains to overlap by a small, fixed, number of fine element layers. In the following section we address this issue in a different manner by proposing a new two level optimal AS preconditioner of the form (2.10), which requires substantially fewer elements in the overlap region as \mathcal{T}^h is refined ($O(h^{-1})$ as $h \rightarrow 0$ as opposed to $O(h^{-2})$). This is achieved by considering a hierarchy of meshes between \mathcal{T}^H and \mathcal{T}^h , each defined by a single level of refinement of its predecessor. Whilst the total overlap between the subdomains remains $O(H)$ in size, at each level of the mesh hierarchy the overlap is the width of just one element. This is illustrated in Figure 1 which shows an overlap of size H in two cases: the first with a uniformly refined mesh in the overlap region, and the second with a mesh which is refined into the overlap region to a width of just one element at each level of the mesh hierarchy.

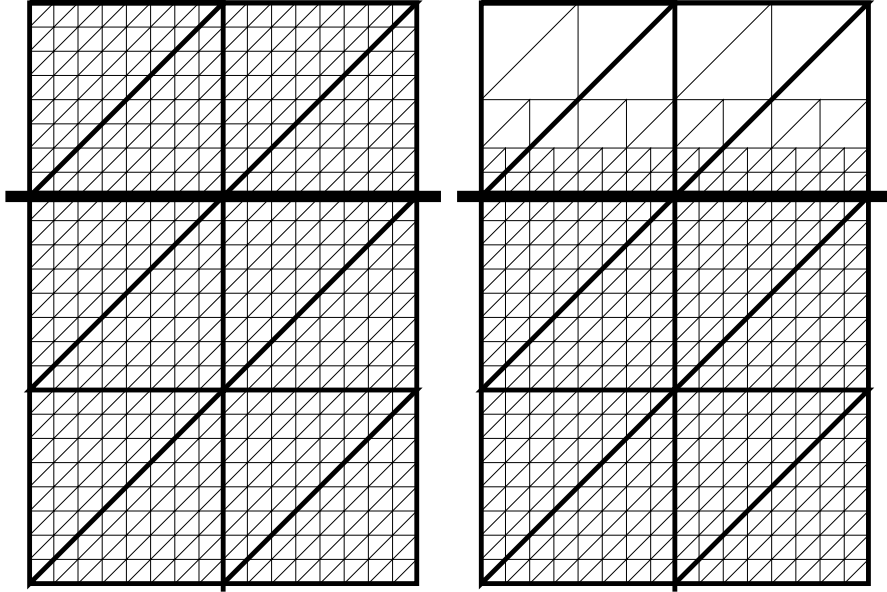


Figure 1: A comparison between a mesh which is uniformly refined in the overlap region (left) and one that is non-uniformly refined in the overlap region (right).

3 A New Preconditioner

In order to describe the domain decomposition preconditioner that we propose in this section it is necessary to begin by establishing some notation. We will again consider (1.1) to (1.3) as a test problem, maintaining the zero Dirichlet boundary conditions for simplicity. Many of the technical details that follow are concerned with ensuring that both the method itself and the analysis that follow are completely general with respect to the domain geometry and how it is decomposed. On first reading however it might be more straightforward to visualize the ideas presented by considering a less than general situation. For this reason we also provide a specific model example using a uniformly refined rectangular domain with a regular Cartesian product decomposition (see Figure 2).

Let \mathcal{T}_0 be a coarse triangulation of Ω consisting of N_0 triangular elements, $\tau_j^{(0)}$, such that $\tau_j^{(0)} = \overline{\tau_j^{(0)}}$,

$$\overline{\Omega} = \bigcup_{j=1}^{N_0} \tau_j^{(0)} \quad \text{and} \quad \mathcal{T}_0 = \{\tau_j^{(0)}\}_{j=1}^{N_0}. \quad (3.1)$$

Also let $\text{diameter}(\tau_j^{(0)}) = O(H)$ (so this triangulation could also be referred to as \mathcal{T}^H in the notation of the previous section), and divide Ω into p *non-overlapping* subdomains Ω_i . These subdomains should be such that:

$$\overline{\Omega} = \bigcup_{i=1}^p \overline{\Omega}_i, \quad (3.2)$$

$$\Omega_i \cap \Omega_j = \emptyset \quad (i \neq j), \quad (3.3)$$

$$\overline{\Omega}_i = \bigcup_{j \in I_i} \tau_j^{(0)} \quad \text{where } I_i \subset \{1, \dots, N_0\} \quad (I_i \neq \emptyset). \quad (3.4)$$

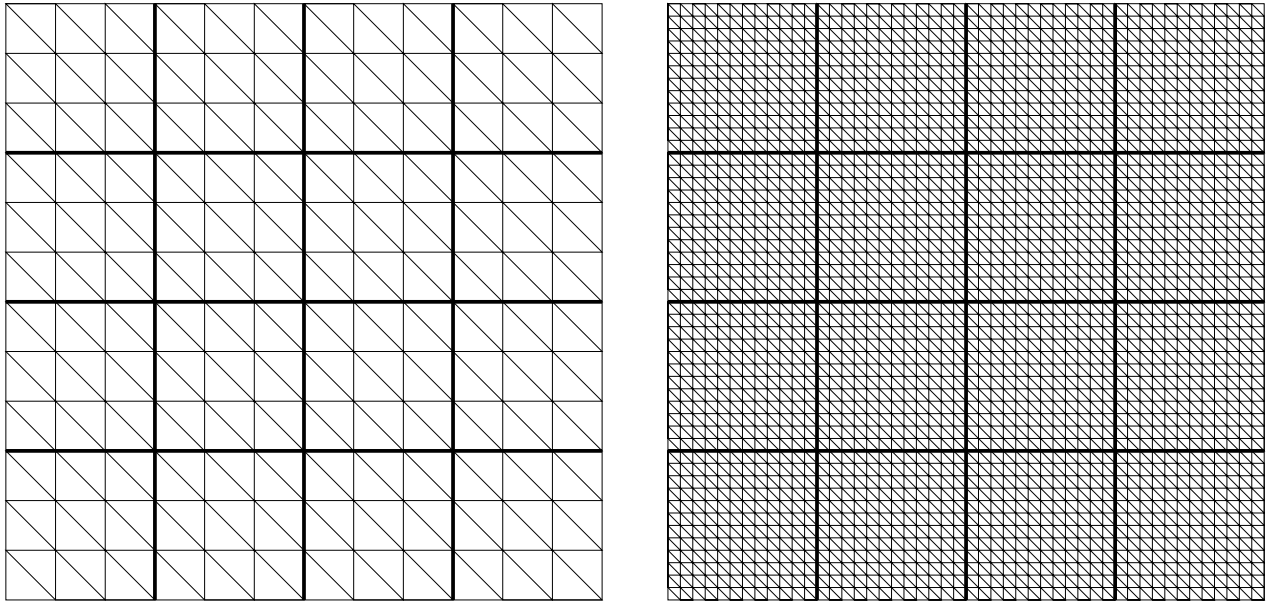


Figure 2: The model example, illustrating a regular Cartesian product decomposition of a simple rectangular domain: coarse grid \mathcal{T}_0 (left) and uniformly refined grid \mathcal{T}_2 (right).

We now permit \mathcal{T}_0 to be refined several times, to produce a family of triangulations, $\mathcal{T}_0, \dots, \mathcal{T}_J$, where each triangulation, \mathcal{T}_k , consists of N_k elements, $\tau_j^{(k)}$, such that

$$\bar{\Omega} = \bigcup_{j=1}^{N_k} \tau_j^{(k)} \quad \text{and} \quad \mathcal{T}_k = \{\tau_j^{(k)}\}_{j=1}^{N_k}. \quad (3.5)$$

The successive mesh refinements that define this sequence of triangulations need not be global and may be non-conforming, however we do require that they satisfy a number of conditions, as in [9] for example:

1. $\tau \in \mathcal{T}_{k+1}$ implies that either
 - (a) $\tau \in \mathcal{T}_k$, or
 - (b) τ has been generated as a refinement of an element of \mathcal{T}_k into four similar children,
2. the level of any triangles which share a common point can differ by at most one,
3. only triangles at level k may be refined in the transition from \mathcal{T}_k to \mathcal{T}_{k+1} .

(Here the level of a triangle is defined to be the least value of k for which that triangle is an element of \mathcal{T}_k .) In addition to the above we will also require that:

4. in the final mesh, \mathcal{T}_J , all pairs of triangles on either side of the boundary of each subdomain Ω_i have the same level as each other.

Note that Figure 2 shows a simple example of such a nested sequence of triangulations for $J = 2$. In this case every triangle in \mathcal{T}_2 is a level 2 triangle and the number of subdomains, p , is 16.

Having defined a decomposition of Ω into subdomains and a nested sequence of triangulations of Ω we next define the restrictions of each of these triangulations onto each subdomain by

$$\Omega_{i,k} = \{\tau_j^{(k)} : \tau_j^{(k)} \subset \bar{\Omega}_i\}. \quad (3.6)$$

In order to introduce a certain amount of overlap between neighbouring subdomains we also define

$$\tilde{\Omega}_{i,k} = \{\tau_j^{(k)} : \tau_j^{(k)} \text{ has a common point with } \bar{\Omega}_i\}. \quad (3.7)$$

Following this we introduce the finite element spaces associated with these local triangulations. Let G be some triangulation and denote by $\mathcal{S}(G)$ the space of continuous piecewise linear functions on G . Then we can make the following definitions:

$$\mathcal{W} = \mathcal{S}(\mathcal{T}_J) \quad (3.8)$$

$$\mathcal{W}_0 = \mathcal{S}(\mathcal{T}_0) \quad (3.9)$$

$$\mathcal{W}_{i,k} = \mathcal{S}(\Omega_{i,k}) \quad (3.10)$$

$$\tilde{\mathcal{W}}_{i,k} = \mathcal{S}(\tilde{\Omega}_{i,k}) \quad (3.11)$$

$$\tilde{\mathcal{W}}_i = \tilde{\mathcal{W}}_{i,0} + \dots + \tilde{\mathcal{W}}_{i,J}. \quad (3.12)$$

It is evident that

$$\mathcal{W} = \mathcal{W}_0 + \tilde{\mathcal{W}}_1 + \dots + \tilde{\mathcal{W}}_p \quad (3.13)$$

and this is the decomposition that we propose for the two level additive Schwarz preconditioner of the form (2.10). Figure 3 illustrates the meshes $\tilde{\Omega}_{i,k}$ that are the basis for the decomposition (3.13) in the case of our regularly decomposed model problem (where i is the number of the top left subdomain and $k = 0, 1$ and 2).

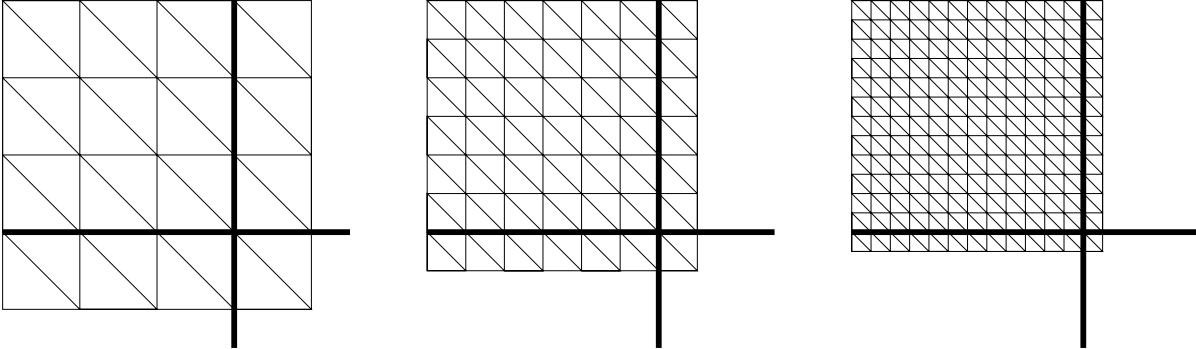


Figure 3: An illustration of $\tilde{\Omega}_{i,0}$ (left), $\tilde{\Omega}_{i,1}$ (centre) and $\tilde{\Omega}_{i,2}$ (right), where subdomain i is the top left subdomain of Figure 2.

In order to prove that this preconditioner is optimal Theorem 2.1 demonstrates that it is sufficient, given any $u^h \in \mathcal{W}$, to provide a construction for $u_0^h \in \mathcal{W}_0$ and $u_i^h \in \tilde{\mathcal{W}}_i$ ($i = 1, \dots, p$) such that

$$u^h = \sum_{i=0}^p u_i^h \quad (3.14)$$

and

$$\sum_{i=0}^p \mathcal{A}_i(u_i^h, u_i^h) \leq C \mathcal{A}(u^h, u^h), \quad (3.15)$$

for some $C > 0$ which is independent of h , H and p . To allow such a construction to be produced it is necessary first to introduce some further notation and then to prove a preliminary lemma.

Given the set of non-overlapping subdomains Ω_i we define a colouring of the Ω_i such that no neighbouring subdomains are the same colour and that the boundary of each subdomain of colour m should have no isolated points in common with the union of the boundary of all subdomains of colour 1 to $m - 1$. Let the number of colours required be n_c , which we assume is independent of h , H and p (although it may be slightly different to ν_c appearing in Theorem 2.1). Figure 4 illustrates an example of a suitable colouring (with $n_c = 4$) for the subdomains defined in Figure 2. It also illustrates a second example which violates the restriction that each subdomain of colour m should have no isolated points in common with the union of the boundary of subdomains of lower numbered colours.

1	2	1	2
3	4	3	4
1	2	1	2
3	4	3	4

3	4	1	2	
1	2	✕	3	4
3	4	1	2	
1	2	✕	3	4

Figure 4: Examples of a valid (left) and an invalid (right) colouring of the subdomains used in the example of Figure 2. The points marked with an X are isolated points on the boundary of subdomains of colour 2 that are also on the boundary of subdomains of colour 1.

Having introduced an appropriate colouring of the subdomains, let $c(i)$ denote the set of indices of those subdomains of colour i (for $i = 1, \dots, n_c$). We may now define

$$\partial\Omega_i = \text{the boundary of } \Omega_i, \quad (3.16)$$

$$\Omega_{c(m)} = \bigcup_{i \in c(m)} \Omega_i, \quad (3.17)$$

$$\partial\Omega_{c(m)} = \text{the boundary of } \Omega_{c(m)} \quad (3.18)$$

and, for each $i \in c(m)$ ($m = 1, \dots, n_c$),

$$\Gamma_i = \partial\Omega_E \cup \left(\partial\Omega_i \cap \left(\bigcup_{n=1}^{m-1} \partial\Omega_{c(n)} \right) \right). \quad (3.19)$$

Figure 5 illustrates these sets Γ_i for our regularly decomposed model problem and the valid colouring shown in Figure 4. Furthermore, with this definition of Γ_i , it is possible to introduce three more

finite element spaces, $\mathcal{W}_{i,k,0}$, $\hat{\mathcal{W}}_{i,k}$ and $\hat{\mathcal{W}}_i$, which are subspaces of $\mathcal{W}_{i,k}$, $\tilde{\mathcal{W}}_{i,k}$ and $\tilde{\mathcal{W}}_i$ respectively:

$$\mathcal{W}_{i,k,0} = \{u_i^h \in \mathcal{W}_{i,k} : u_i^h(\underline{x}) = 0 \ \forall \underline{x} \in \Gamma_i\}, \quad (3.20)$$

$$\hat{\mathcal{W}}_{i,k} = \mathcal{S}(\hat{\Omega}_{i,k}), \quad (3.21)$$

and

$$\hat{\mathcal{W}}_i = \hat{\mathcal{W}}_{i,0} + \dots + \hat{\mathcal{W}}_{i,J}, \quad (3.22)$$

where

$$\hat{\Omega}_{i,k} = \left\{ \bigcup_j \tau_j^{(k)} : \tau_j^{(k)} \text{ has a common point with } \bar{\Omega}_i - \Gamma_i \right\}. \quad (3.23)$$

Also, let $\hat{\Omega}_i$ be the subset of Ω which is covered by the triangulation $\hat{\Omega}_{i,0}$. Figure 6 illustrates the meshes $\hat{\Omega}_{i,k}$ for one specific choice of i using the first colouring shown in Figure 4. Note that this construction is such that overlap from subdomain i is only allowed to occur into subdomains with a larger numbered colour than the colour of subdomain i : see Figure 5.

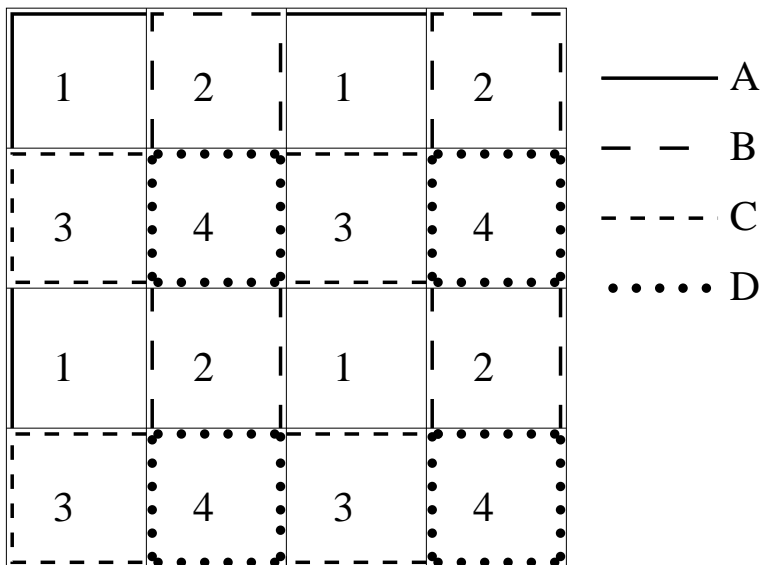


Figure 5: An illustration of Γ_i for the valid colouring shown in Figure 4: line A is $\cup_{i \in c(1)} \Gamma_i \cap \bar{\Omega}_i$; line B is $\cup_{i \in c(2)} \Gamma_i \cap \bar{\Omega}_i$; line C is $\cup_{i \in c(3)} \Gamma_i \cap \bar{\Omega}_i$; line D is $\cup_{i \in c(4)} \Gamma_i \cap \bar{\Omega}_i$.

We are now ready to define a mechanism for extending an arbitrary function $w_i^h \in \mathcal{W}_{i,J,0}$ to $\hat{\mathcal{W}}_i$, as follows. In defining this mechanism note that the vertices of $\hat{\Omega}_{i,k} - \bar{\Omega}_{i,k}$ are easily identified in the example shown in Figure 6.

Algorithm 3.1 Let $w_i^h \in \mathcal{W}_{i,J,0}$. Let $Q_{i,k} : \mathcal{L}^2(\Omega_i) \rightarrow \mathcal{W}_{i,k,0}$ be the usual \mathcal{L}^2 orthogonal projection onto $\mathcal{W}_{i,k,0}$ and define

$$v_{i,0}^h = Q_{i,0} w_i^h \quad \text{and} \quad v_{i,k}^h = (Q_{i,k} - Q_{i,k-1}) w_i^h \quad \text{for } k = 1, \dots, J. \quad (3.24)$$

Now denote by $\hat{v}_{i,k}^h \in \hat{\mathcal{W}}_{i,k}$ the extension of $v_{i,k}^h$ which is zero at all vertices of $\hat{\Omega}_{i,k} - \bar{\Omega}_{i,k}$, so it easily follows that

$$\|\hat{v}_{i,k}^h\|_{\mathcal{L}^2(\hat{\Omega}_{i,k})}^2 \leq C_0 \|v_{i,k}^h\|_{\mathcal{L}^2(\Omega_i)}^2 \quad (3.25)$$

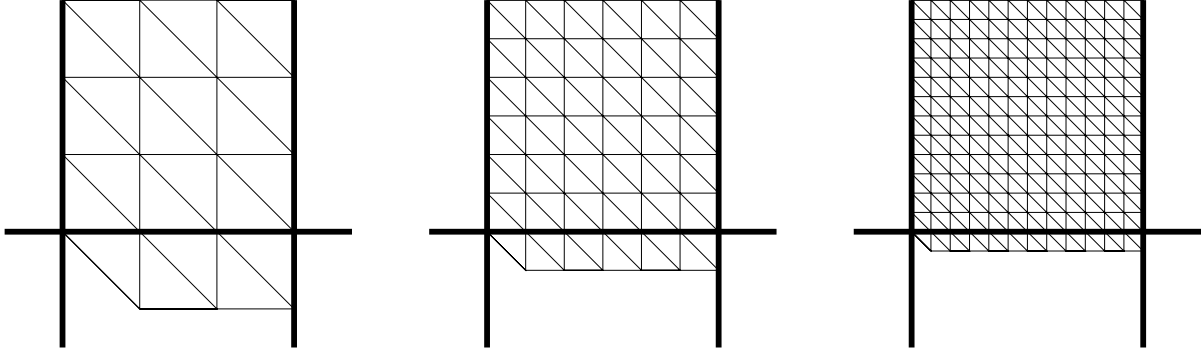


Figure 6: An illustration of $\hat{\Omega}_{i,0}$ (left), $\hat{\Omega}_{i,1}$ (centre) and $\hat{\Omega}_{i,2}$ (right), where subdomain i is the subdomain in the top row and second column of Figures 2 and 5 (i.e. of colour number 2).

for some $C_0 > 0$ which is independent of h , H and p . We are now in a position to define

$$\hat{v}_i^h = \hat{v}_{i,0}^h + \dots + \hat{v}_{i,J}^h, \quad (3.26)$$

which is the required local extension of $w_i^h \in \mathcal{W}_{i,J,0}$ to $\hat{\mathcal{W}}_i$.

Lemma 3.1 *Given $w_i^h \in \mathcal{W}_{i,J,0}$ let $\hat{v}_i^h \in \hat{\mathcal{W}}_i$ be the extension of w_i^h defined by Algorithm 3.1 above. Then there exists $C_1 > 0$, which is independent of h , H and p , such that*

$$\|\hat{v}_i^h\|_{\mathcal{H}^1(\hat{\Omega}_i)}^2 \leq C_1 \left\{ \frac{1}{H^2} \|w_i^h\|_{\mathcal{L}^2(\Omega_i)}^2 + |w_i^h|_{\mathcal{H}^1(\Omega_i)}^2 \right\}. \quad (3.27)$$

Proof First we introduce the following change of variables:

$$x = H s, \quad y = H t; \quad (x, y) \in \Omega_i. \quad (3.28)$$

Under this transformation the domain Ω_i is the image of a domain Ω'_i whose geometric properties are independent of H in the (s, t) plane. Furthermore

$$\frac{1}{H^2} \|w_i^h(x, y)\|_{\mathcal{L}^2(\Omega_i)}^2 + |w_i^h(x, y)|_{\mathcal{H}^1(\Omega_i)}^2 = \|w_i^h(s, t)\|_{\mathcal{L}^2(\Omega'_i)}^2 + |w_i^h(s, t)|_{\mathcal{H}^1(\Omega'_i)}^2, \quad (3.29)$$

and we may define by $Q'_{i,k}$ the projection in the (s, t) variables which corresponds to $Q_{i,k}$. From [9] it follows that there exists $C_2 > 0$, which is independent of h , H and p , such that:

$$\begin{aligned} \frac{1}{H^2} \sum_{k=0}^J 4^k \|v_{i,k}^h\|_{\mathcal{L}^2(\Omega_i)}^2 &= \frac{1}{H^2} \left(\|Q_{i,0} w_i^h(x, y)\|_{\mathcal{L}^2(\Omega_i)}^2 + \sum_{k=1}^J 4^k \|(Q_{i,k} - Q_{i,k-1}) w_i^h(x, y)\|_{\mathcal{L}^2(\Omega_i)}^2 \right) \\ &= \|Q'_{i,0} w_i^h(s, t)\|_{\mathcal{L}^2(\Omega'_i)}^2 + \sum_{k=1}^J 4^k \|(Q'_{i,k} - Q'_{i,k-1}) w_i^h(s, t)\|_{\mathcal{L}^2(\Omega'_i)}^2 \\ &\leq C_2 \|w_i^h(s, t)\|_{\mathcal{H}^1(\Omega'_i)}^2 \\ &= C_2 \left(\frac{1}{H^2} \|w_i^h(x, y)\|_{\mathcal{L}^2(\Omega_i)}^2 + |w_i^h(x, y)|_{\mathcal{H}^1(\Omega_i)}^2 \right). \end{aligned} \quad (3.30)$$

A second inequality that we require comes from [26], where it is shown that there exists $C_3 > 0$, which is independent of h , H and p , such that

$$\begin{aligned} \|\hat{v}_i^h(x, y)\|_{\mathcal{H}^1(\hat{\Omega}_i)}^2 &= H^2 \|\hat{v}_i^h(s, t)\|_{\mathcal{L}^2(\hat{\Omega}'_i)}^2 + |\hat{v}_i^h(s, t)|_{\mathcal{H}^1(\hat{\Omega}'_i)}^2 \\ &\leq C_3 \inf_{\substack{\hat{v}_i^h = \hat{\xi}_0 + \dots + \hat{\xi}_J \\ (\hat{\xi}_k \in \hat{\mathcal{W}}'_{i,k})}} \sum_{k=0}^J 4^k \|\hat{\xi}_k\|_{\mathcal{L}^2(\hat{\Omega}'_i)}^2, \end{aligned} \quad (3.31)$$

where $\hat{\mathcal{W}}'_{i,k}$ is the space which corresponds to $\hat{\mathcal{W}}_{i,k}$ with the change of variables (3.28). From this, along with (3.25) and (3.30), it follows that

$$\begin{aligned} \|\hat{v}_i^h(x, y)\|_{\mathcal{H}^1(\hat{\Omega}_i)}^2 &\leq C_3 \sum_{k=0}^J 4^k \|\hat{v}_{i,k}^h\|_{\mathcal{L}^2(\hat{\Omega}'_i)}^2 \\ &= \frac{C_3}{H^2} \sum_{k=0}^J 4^k \|\hat{v}_{i,k}^h\|_{\mathcal{L}^2(\hat{\Omega}_{i,k})}^2 \\ &\leq \frac{C_0 C_3}{H^2} \sum_{k=0}^J 4^k \|v_{i,k}^h\|_{\mathcal{L}^2(\Omega_i)}^2 \\ &\leq C_0 C_2 C_3 \left(\frac{1}{H^2} \|w_i^h\|_{\mathcal{L}^2(\Omega_i)}^2 + |w_i^h|_{\mathcal{H}^1(\Omega_i)}^2 \right). \end{aligned} \quad (3.32)$$

as required. ///

This lemma forms the main component of our proof that the proposed splitting is stable. The following theorem completes this proof by explicitly constructing a suitable decomposition of any $u^h \in \mathcal{W}$. It should be noted that the proof of the theorem holds for an arbitrary partition of Ω into subdomains Ω_i and could certainly be simplified if less general partitions (e.g. into strips or regular blocks) were considered. For the completely general case it is necessary to introduce a small amount of additional notation. For $m \in \{1, \dots, n_c\}$ let

$$\mathcal{W}_0^{(m)} = \{u^H \in \mathcal{W}_0 : u^H(\underline{x}) = 0 \quad \forall \underline{x} \in \bigcup_{n=1}^{m-1} \Omega_{c(n)}\} \quad (3.33)$$

and $Q_0^{(m)} : \mathcal{L}^2(\Omega) \rightarrow \mathcal{W}_0^{(m)}$ be the \mathcal{L}^2 orthogonal projection onto $\mathcal{W}_0^{(m)}$ given by

$$\int_{\Omega} (Q_0^{(m)} u) w_0^{(m)} d\underline{x} = \int_{\Omega} u w_0^{(m)} d\underline{x} \quad \forall w_0^{(m)} \in \mathcal{W}_0^{(m)}. \quad (3.34)$$

Hence, by the \mathcal{H}^1 stability of the \mathcal{L}^2 projection we have

$$\|Q_0^{(m)} u^h\|_{\mathcal{H}^1(\Omega)} \leq C_4 \|u^h\|_{\mathcal{H}^1(\Omega)}, \quad (3.35)$$

and using standard finite element interpolation estimates we have

$$\frac{1}{H} \|u^h - Q_0^{(m)} u^h\|_{\mathcal{L}^2(\Omega)} + |u^h - Q_0^{(m)} u^h|_{\mathcal{H}^1(\Omega)} \leq C_4 \|u^h\|_{\mathcal{H}^1(\Omega)}, \quad (3.36)$$

for some $C_4 > 0$ which is independent of h , H and p . (Note that, in the case $m = 1$, $\mathcal{W}_0^{(1)} = \mathcal{W}_0$ and $Q_0^{(1)} = Q_0$ as defined in Section 2 above.)

Theorem 3.2 *There exists $C > 0$, which is independent of h , H and p , such that for any $u^h \in \mathcal{W}$ there are $u^H \in \mathcal{W}_0$ and $u_i \in \tilde{\mathcal{W}}_i$ ($i = 1, \dots, p$) such that*

$$u^h = u^H + u_1^h + \dots + u_p^h \quad (3.37)$$

and

$$\|u^H\|_{\mathcal{H}^1(\Omega)}^2 + \|u_1^h\|_{\mathcal{H}^1(\Omega)}^2 + \dots + \|u_p^h\|_{\mathcal{H}^1(\Omega)}^2 \leq C \|u^h\|_{\mathcal{H}^1(\Omega)}^2. \quad (3.38)$$

Proof Given any $u^h \in \mathcal{W}$, we now construct functions $u^H \in \mathcal{W}_0$ and $u_i^h \in \hat{\mathcal{W}}_i \subset \tilde{\mathcal{W}}_i$ (for $i = 1, \dots, p$) such that (3.37) and (3.38) are satisfied.

Let $r_1^h = u^h$.

Let $u_1^H = Q_0^{(1)} r_1^h$.

Let $w_1^h = r_1^h - u_1^H$.

Let $[w_1^h]_{\Omega_i}$ be the restriction of w_1^h to Ω_i .

For each $i \in c(1)$:

use Algorithm 3.1 to define $u_i^h \in \hat{\mathcal{W}}_i$ to be the extension of $[w_1^h]_{\Omega_i}$.

For $m = 2$ to n_c .

Let $r_m^h = w_{m-1}^h - \sum_{j \in c(m-1)} u_j^h$ (hence $r_m^h(\underline{x}) = 0 \quad \forall \underline{x} \in \bigcup_{n=1}^{m-1} \Omega_{c(n)}$).

Let $u_m^H = Q_0^{(m)} r_m^h$.

Let $w_m^h = r_m^h - u_m^H$.

Let $[w_m^h]_{\Omega_i}$ be the restriction of w_m^h to Ω_i (hence $[w_m^h]_{\Omega_i} \in \mathcal{W}_{i,J,0}$).

For each $i \in c(m)$:

use Algorithm 3.1 to define $u_i^h \in \hat{\mathcal{W}}_i$ to be the extension of $[w_m^h]_{\Omega_i}$.

Let $u^H = u_1^H + \dots + u_{n_c}^H$.

Note that in the above definitions, when $i \in c(n_c)$ the functions u_i are just the restrictions of $w_{n_c}^h$ to Ω_i since the extension operation is just the identity in this case (because $\Gamma_i = \partial\Omega_i$ for $i \in c(n_c)$ and so $\hat{\Omega}_{i,k} = \Omega_{i,k}$ and $\hat{\mathcal{W}}_{i,k} = \mathcal{W}_{i,k}$ for $k = 1, \dots, J$). For these definitions of u^H and u_i^h (for $i = 1, \dots, p$) we now prove that (3.37) and (3.38) both hold.

To prove (3.37) first let $\underline{x} \in \Omega_i$ for $i \in c(1)$. Then

$$\begin{aligned} u^H + u_1^h + \dots + u_p^h &= \sum_{n=1}^{n_c} u_n^H(\underline{x}) + \sum_{j=1}^p u_j^h(\underline{x}) \\ &= u_1^H(\underline{x}) + u_i^h(\underline{x}) \\ &= u_1^H(\underline{x}) + w_1^h(\underline{x}) \\ &= r_1^h \\ &= u^h. \end{aligned}$$

Now let $\underline{x} \in \Omega_i$ for $i \in c(m)$ for any $m \in \{2, \dots, n_c\}$. Then

$$\begin{aligned} u^H + u_1^h + \dots + u_p^h &= \sum_{n=1}^{n_c} u_n^H(\underline{x}) + \sum_{j=1}^p u_j^h(\underline{x}) \\ &= \sum_{n=1}^m \left(u_n^H(\underline{x}) + \sum_{j \in c(n)} u_j^h(\underline{x}) \right) \\ &= \sum_{n=1}^{m-1} \left(u_n^H(\underline{x}) + \sum_{j \in c(n)} u_j^h(\underline{x}) \right) + u_m^H(\underline{x}) + u_i^h(\underline{x}) \end{aligned}$$

$$\begin{aligned}
&= \sum_{n=1}^{m-1} \left(u_n^H(\underline{x}) + \sum_{j \in c(n)} u_j^h(\underline{x}) \right) + u_m^H(\underline{x}) + w_m^h(\underline{x}) \\
&= \sum_{n=1}^{m-1} \left(u_n^H(\underline{x}) + \sum_{j \in c(n)} u_j^h(\underline{x}) \right) + r_m^h(\underline{x}) \\
&= \sum_{n=1}^{m-1} \left(u_n^H(\underline{x}) + \sum_{j \in c(n)} u_j^h(\underline{x}) \right) + r_{m-1}^h(\underline{x}) - u_{m-1}^H(\underline{x}) - \sum_{j \in c(m-1)} u_j^h \\
&= \sum_{n=1}^{m-2} \left(u_n^H(\underline{x}) + \sum_{j \in c(n)} u_j^h(\underline{x}) \right) + r_{m-1}^h(\underline{x}) \\
&= \sum_{n=1}^{m-3} \left(u_n^H(\underline{x}) + \sum_{j \in c(n)} u_j^h(\underline{x}) \right) + r_{m-2}^h(\underline{x}) \\
&= : \\
&= \left(u_1^H(\underline{x}) + \sum_{j \in c(1)} u_j^h(\underline{x}) \right) + r_2^h(\underline{x}) \\
&= r_1^h \\
&= u^h.
\end{aligned}$$

Finally, we observe that if \underline{x} is on the boundary between two or more subdomains, then the above argument may be applied to the subdomain of the lowest colour to show that $u^H + u_1^h + \dots + u_p^h = u^h$ at this point too. (This argument uses the continuity of each w_m^h and the fact that $w_m^h(\underline{x}) = 0$ for each subdomain m whose boundary contains \underline{x} , except the one with the lowest colour.)

To conclude the proof we now demonstrate that (3.38) also holds. In order to do this first note that, since $\cup_{m=1}^{n_c} c(m) = \{1, \dots, p\}$ and $u^H = \sum_{m=1}^{n_c} u_m^H$,

$$\|u^H\|_{\mathcal{H}^1(\Omega)}^2 + \|u_1^h\|_{\mathcal{H}^1(\Omega)}^2 + \dots + \|u_p^h\|_{\mathcal{H}^1(\Omega)}^2 \leq \sum_{m=1}^{n_c} \left(\|u_m^H\|_{\mathcal{H}^1(\Omega)}^2 + \sum_{i \in c(m)} \|u_i^h\|_{\mathcal{H}^1(\Omega)}^2 \right). \quad (3.39)$$

Hence, since n_c is assumed to be independent of h , H and p , it is sufficient to show that

$$\|u_m^H\|_{\mathcal{H}^1(\Omega)}^2 + \sum_{i \in c(m)} \|u_i^h\|_{\mathcal{H}^1(\Omega)}^2 \leq C \|u^h\|_{\mathcal{H}^1(\Omega)}^2 \quad (3.40)$$

for some C which is independent of h , H and p , and any $m \in \{1, \dots, n_c\}$. Let the quantity on the left-hand side of (3.40) be S_m , say. Then

$$\begin{aligned}
S_m &= \|u_m^H\|_{\mathcal{H}^1(\Omega)}^2 + \sum_{i \in c(m)} \|u_i^h\|_{\mathcal{H}^1(\hat{\Omega}_i)}^2 \\
&\quad (\text{since } u_i^h \in \hat{\mathcal{W}}_i) \\
&\leq C_4 \|r_m^h\|_{\mathcal{H}^1(\Omega)}^2 + \sum_{i \in c(m)} \|u_i^h\|_{\mathcal{H}^1(\hat{\Omega}_i)}^2 \\
&\quad (\text{using (3.35)}) \\
&\leq C_4 \|r_m^h\|_{\mathcal{H}^1(\Omega)}^2 + C_1 \sum_{i \in c(m)} \left\{ \frac{1}{H^2} \|w_m^h\|_{\mathcal{L}^2(\Omega_i)}^2 + |w_m^h|_{\mathcal{H}^1(\Omega_i)}^2 \right\}
\end{aligned}$$

$$\begin{aligned}
& \text{(using Lemma 3.1)} \\
\leq & C_4 \|r_m^h\|_{\mathcal{H}^1(\Omega)}^2 + C_1 C_4^2 \sum_{i \in c(m)} \|r_m^h\|_{\mathcal{H}^1(\Omega_i)}^2 \\
& \text{(using (3.36))} \\
= & C_4 \|r_m^h\|_{\mathcal{H}^1(\Omega)}^2 + C_1 C_4^2 \|r_m^h\|_{\mathcal{H}^1(\Omega)}^2 \\
= & C_5 \|r_m^h\|_{\mathcal{H}^1(\Omega)}^2 .
\end{aligned} \tag{3.41}$$

Clearly if $m = 1$ then $r_m^h = u^h$ and we are done. Otherwise note that

$$\begin{aligned}
S_m & \leq C_5 \|r_m^h\|_{\mathcal{H}^1(\Omega)}^2 \\
& \leq C_5 \left(\|r_{m-1}^h\|_{\mathcal{H}^1(\Omega)}^2 + S_{m-1} \right) \\
& \leq C_5 \left(\|r_{m-1}^h\|_{\mathcal{H}^1(\Omega)}^2 + C_5 \|r_{m-1}^h\|_{\mathcal{H}^1(\Omega)}^2 \right) \\
& \quad \text{(using the same argument as in (3.41) above)} \\
& = C_6 \|r_{m-1}^h\|_{\mathcal{H}^1(\Omega)}^2 \\
& \leq C_7 \|r_1^h\|_{\mathcal{H}^1(\Omega)}^2 \\
& \quad \text{(repeating this argument } m - 2 \text{ further times)} \\
& = C_7 \|u^h\|_{\mathcal{H}^1(\Omega)}^2 ,
\end{aligned}$$

as required. ///

Having demonstrated that the splitting given by (3.13) is stable it is now a simple matter to invoke Theorem 2.1 (with ν_c replaced by $\nu_c + 1$ to take into account the coarse grid space \mathcal{W}_0) and the equivalence of the norm $\mathcal{A}(\cdot, \cdot)^{1/2}$ with the \mathcal{H}^1 norm, to deduce that the corresponding additive Schwarz preconditioner is optimal.

The results of this section show that, in two dimensions, it is possible to obtain an optimal two level AS preconditioner with an overlap which contains $O(h^{-1})$ elements only, provided appropriate use is made of the mesh hierarchy. Whilst the proofs developed here are fully general in terms of subdomain shapes and connectivity a simple, more regular, example has also been included for illustrative purposes. In contrasting these results with more standard theoretical results (as in the following section), which require $O(h^{-2})$ elements in the overlap regions for optimality, a number of practical points should be noted. Firstly, as described in [30] for example, the standard two level AS method does not use a generous overlap in practice. Typically, two to four fine mesh layers are found to be most economical. It follows therefore that the weakly overlapping approach that we have analysed will not generally be any less (or more) computationally expensive per iteration than standard two level AS solvers. What our approach does offer however is the guarantee of optimality; which does not hold when only a fixed number of fine grid layers of overlap are used. Furthermore, the communication cost at each iteration is $O(h^{-1})$ in both cases and the weakly overlapping approach has the added simplicity of not requiring any trade-off between cost per iteration (i.e. overlap size) and the total iteration count to be considered. Secondly, when the weakly overlapping approach is applied to an arbitrary decomposition of Ω , the fact that only a single layer of overlap is required at each mesh level makes its implementation extremely straightforward. This is arguably less complex than the implementation of a more standard approach where four (say) layers of elements are required in the overlap: which can be quite cumbersome to calculate on a geometrically complex decomposition.

4 Numerical Examples

In this section we present a small number of two-dimensional numerical examples which demonstrate the efficiency of the preconditioner introduced above. For these examples we make a slight modification to the preconditioner so as to allow the practical parallel generation of the partitioned hierarchical meshes that are required.

In this modified algorithm, once the coarse mesh \mathcal{T}_0 has been partitioned into the p non-overlapping subdomains, Ω_i , p copies of it are made. Copy i is then refined only in $\tilde{\Omega}_{i,k}$ at level k of the refinement process. The continuous piecewise linear finite element spaces on the resulting meshes are then

$$\mathcal{U}_i = \mathcal{W}_0 \cup \tilde{\mathcal{W}}_i \quad (4.1)$$

for $i = 1, \dots, p$. The following corollary follows immediately from Theorem 3.2.

Corollary 4.1 *Let the spaces \mathcal{U}_i be given by (4.1) for $i = 1, \dots, p$. Then*

$$\mathcal{W} = \mathcal{U}_1 + \dots + \mathcal{U}_p \quad (4.2)$$

is also a stable decomposition.

The advantages of this approach are outlined in some detail in [4] where it is shown that parallel adaptive mesh generation may be achieved in a well load-balanced manner. The main disadvantage is that one is effectively completing a coarse mesh solve as part of *each* subspace correction (i.e. p times per iteration) rather than once per iteration. However, in many practical parallel codes (e.g. [22]) the coarse grid solve is completed sequentially on a single processor anyway, so the overhead of repeating it on all p processors simultaneously is not necessarily that great.

The other minor practical modification that we have made to the preconditioner outlined in the previous section comes from the use of transition (sometimes known as “green” [29]) elements in our meshes in order to keep them conforming. In Figure 1 it may be observed that there are a number of “slave” nodes in the non-uniformly refined mesh which cause the mesh shown to be non-conforming. The solution values at these nodes are not free: they are determined by the nodal values at the ends of the edges on which the slave nodes lie. For a practical implementation it turns out to be much simpler to allow the solution values at these nodes to be free by bisecting the element on the unrefined side of the edge that has the “hanging” node on it. This is the approach that is used in the examples below.

For the first two test problems considered, sequences of uniformly refined meshes, \mathcal{T}_k , have been used.

Problem 4.1

$$\begin{aligned} -\underline{\nabla} \cdot (\underline{\nabla} u) &= f \quad \forall \underline{x} \in \Omega \equiv (0, 1) \times (0, 1), \\ u &= g \quad \forall \underline{x} \in \partial\Omega. \end{aligned}$$

Problem 4.2

$$\begin{aligned} -\underline{\nabla} \cdot \left(\begin{pmatrix} 10^2 & 0 \\ 0 & 1 \end{pmatrix} \underline{\nabla} u \right) &= f \quad \forall \underline{x} \in \Omega \equiv (0, 1) \times (0, 1), \\ u &= g \quad \forall \underline{x} \in \partial\Omega. \end{aligned}$$

In each case f has been chosen to permit the exact solution $u = g$ for a quadratic choice of g .

Tables 1 and 2 below show the number of iterations required by both the conventional optimal (as defined by (2.10) and Theorem 2.2) and the new two level additive Schwarz preconditioners in order to reduce the 2-norm of the initial residual by a factor of 10^6 for these two problems respectively. In each case a 256 element coarse mesh has been used and the final fine grids have between 4096 and 1048576 elements. The number of subdomains goes from 2 to 16 and for the purposes of these comparisons the local solves on each subproblem are exact (but see below for a discussion of this).

Fine mesh	Conventional AS	New AS	CPU Ratio	p
4096	6	6	1.0	2
16384	6	6	0.85	
65536	6	6	0.57	
262144	6	6	0.47	
1048576	6	6	0.35	
4096	8	9	1.0	4
16384	8	8	0.65	
65536	8	8	0.56	
262144	8	7	0.42	
1048576	8	7	0.27	
4096	13	12	0.88	8
16384	13	12	0.68	
65536	12	12	0.52	
262144	11	11	0.36	
1048576	11	11	0.29	
4096	14	14	0.73	16
16384	14	13	0.58	
65536	14	13	0.44	
262144	14	12	0.30	
1048576	13	12	0.25	

Table 1: The number of iterations required to reduce the 2-norm of the residual by a factor of 10^6 using the two different AS preconditioners when solving Problem 4.1 using piecewise linear finite elements. Column 4 shows the relative speed of the New versus the Conventional optimal two level preconditioner.

Inspection of these tables shows that there is very little to choose between the number of iterations required by the conventional optimal AS preconditioner with, $O(h^{-2})$ elements in the overlap regions, and the new preconditioner, with just $O(h^{-1})$ elements in the overlap regions. This is an important observation since it indicates that the splitting constant, C , is of approximately the same size for the new splitting as for the conventional two level splitting with a generous overlap. Indeed, it is the significance of this observation that motivates our comparison between the two approaches. Full details of the practical parallel implementation of the preconditioners is beyond the scope of this paper (but see [5] for a complete description of our parallel implementation). Nevertheless, the relative timings when using one subdomain per processor are also included in Tables 1 and 2 in order to illustrate the advantages of the weakly overlapping approach. It is noticeable that the significant reduction in the size of the subproblems that must be solved at each iteration of the new algorithm, due to the smaller number of elements in the overlap region, clearly leads to a reduced

Fine mesh	Conventional AS	New AS	CPU Ratio	p
4096	7	8	1.0	2
16384	7	8	0.82	
65536	7	8	0.69	
262144	7	8	0.49	
1048576	7	8	0.46	
4096	11	12	1.0	4
16384	12	13	0.74	
65536	12	13	0.66	
262144	11	12	0.50	
1048576	10	12	0.30	
4096	14	15	0.90	8
16384	14	16	0.67	
65536	13	16	0.65	
262144	13	17	0.53	
1048576	13	17	0.39	
4096	18	19	0.71	16
16384	18	19	0.60	
65536	19	20	0.58	
262144	18	21	0.41	
1048576	18	21	0.31	

Table 2: The number of iterations required to reduce the 2-norm of the residual by a factor of 10^6 using the two different AS preconditioners when solving Problem 4.2 using piecewise linear finite elements. Column 4 shows the relative speed of the New versus the Conventional optimal two level preconditioner.

parallel solution time. Unsurprisingly this reduction becomes more significant the more the mesh is refined.

It should also be noted at this point that the results of Tables 1 and 2 do show an increase in the number of iterations required as p , the number of subdomains, is increased (for both versions of the algorithm). This may be accounted for by the fact that n_c increases as p increases from 2 to 8, and that for the relatively small values of p considered here (up to $p = 16$) the asymptotic limit has not yet been reached, even though n_c is at most 5 in all cases. It may be observed however that the growth in the number of iterations as p increases is already beginning to slow down as p goes from 8 to 16. Also, the iteration counts for Problem 4.2 are greater than those for corresponding solutions of Problem 4.1. This may be accounted for in the theory of the previous section by noting that the norm equivalence $\mathcal{A}(\cdot, \cdot)^{1/2} \sim \mathcal{H}^1$ will involve a larger ratio of constants in the upper and lower bounds for Problem 4.2 than Problem 4.1.

In practice it is not necessary to solve the subproblems involving the matrices A_i in (2.10) exactly in order to maintain the optimality of the preconditioner. This is discussed in some detail elsewhere (see, for example, [11, 36]) and so we merely comment that our numerical experiments suggest that reducing the residual by a factor of between 10^1 and 10^2 when “solving” these subproblems appears to provide a good balance between allowing a small increase in the total number of iterations and keeping the cost of each iteration as low as possible. For the examples in this section we have applied a preconditioned conjugate gradient solver with an algebraic preconditioner based upon an

incomplete factorization of A_i (see [6, 7] for example).

We conclude this section by demonstrating the effectiveness of the preconditioner for a locally, rather than uniformly, refined mesh.

Problem 4.3

$$\begin{aligned} -\underline{\nabla} \cdot (\underline{\nabla} u) &= f \quad \forall \underline{x} \in \Omega \equiv (0, 1) \times (0, 1) , \\ u &= g \quad \forall \underline{x} \in \partial\Omega . \end{aligned}$$

Where f and g are now chosen so that the analytic solution is given by:

$$u = (1 - (2x_1 - 1)^{100})(1 - (2x_2 - 1)^{100}) \quad \forall \underline{x} \in \Omega . \tag{4.3}$$

Note that this solution is unity in the interior of Ω but tends to zero very rapidly in a thin layer (of width ≈ 0.02) near to the boundary; allowing the Dirichlet condition $u = 0$ to be satisfied throughout $\partial\Omega$.

When solving this problem we again use a coarse triangulation which contains just 256 elements, divided into 2, 4, 8 and 16 subdomains. Note that for this example it is only appropriate to refine the mesh in the boundary layer, where the solution changes from one to zero, and four such sets of results are presented in Table 3: corresponding to 5, 6, 7 and 8 levels of refinement in the layer (for the purposes of these tests the local refinement of an element is triggered when the exact interpolation error on that element is greater than 10^{-10} (2-norm) unless the element is already at the maximum refinement level). In each case the coarse mesh \mathcal{T}_0 has been partitioned in such a way that the number of elements in the final mesh, \mathcal{T}_J , in each subregion is approximately equal. In the cases where $p = 8$ and $p = 16$ this means that there are differing numbers of coarse elements in each subregion (between 8 and 40 when $p = 16$ for example) — the partitions into 2 or 4 may be computed more simply however, using the symmetry of the problem and the coarse mesh (see Fig. 7 for example). As with Tables 1 and 2, the results of Table 3 clearly show independence from h for a sufficient level of refinement, however the independence from p is not yet evident for the small values considered (up to $p = 16$): although we again see a reduction in the growth of the number of iterations as p increases.

Refinements (Elements/Vertices)	$p = 2$	$p = 4$	$p = 8$	$p = 16$
5 (48680/24853)	7	9	13	18
6 (145088/73569)	7	10	15	18
7 (362272/184685)	8	10	16	18
8 (543632/275913)	8	10	16	19

Table 3: The number of iterations required to reduce the 2-norm of the residual by a factor of 10^6 using the new AS preconditioner when solving Problem 4.3 using piecewise linear finite elements.

As well as verifying our theoretical results in the case of a locally refined mesh, the last example also illustrates the potential of the technique for use within truly adaptive algorithms, based upon *a posteriori* error estimates and local refinement (see [1, 35] for example). Such algorithms are not without their difficulties however since undertaking adaptivity in parallel presents challenging dynamic load-balancing problems (e.g. [32]) which clearly cannot be dealt with using the simple *a priori* partitioning approach taken above. For one possible means of overcoming these problems we refer the reader to [4], where a paradigm is presented in which the *a posteriori* error estimates

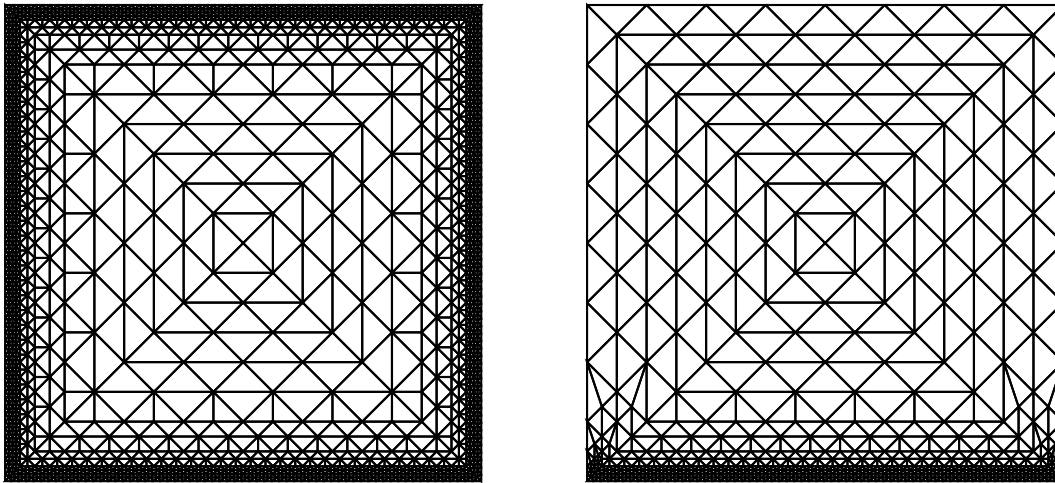


Figure 7: The overall refined mesh (left) and a typical mesh on one processor when $p = 4$ (right) for Problem 4.3. Here the coarse mesh contains 256 elements and, for this illustration, at most three levels of refinement are permitted.

are themselves used to assist with load-balancing. We also note the additional theoretical issue of selecting an appropriate definition for h , the mesh size parameter, for locally refined meshes. Whilst this does not affect the theoretical results presented in this paper it does have an important bearing on quantitative overhead estimates in terms of the problem size.

5 Extension to Three Dimensions

So far, for reasons of clarity and simplicity, our discussion has been restricted to problems of the form (1.1) – (1.3) in two dimensions. In this section we demonstrate that both the theoretical results and the practical realization may be successfully generalized to three dimensions. Again we consider problems of the form (1.1) – (1.3) but now we allow $\Omega \subset \mathbb{R}^3$. We will assume that Ω may be covered by a set of tetrahedra, \mathcal{T}_0 , consisting of N_0 tetrahedral elements $\tau_j^{(0)}$ ($j = 1, \dots, N_0$). In order to refine a tetrahedron we use the standard approach of bisecting each edge to produce 8 children, as shown in Figure 8. Note that although the children are not generally geometrically similar their aspect ratios are always bounded independently of h . Full details of the refinement algorithm may be found in [31].

Using the above refinement strategy it is possible to generate a family of three-dimensional triangulations, $\mathcal{T}_0, \dots, \mathcal{T}_J$, satisfying the same restrictions as the two-dimensional family introduced in Section 3 (with the obvious modification to condition 1(b) for eight children). From this, the spaces \mathcal{W} , $\mathcal{W}_{i,k,0}$ ($k = 1, \dots, J$) and $\hat{\mathcal{W}}_i$, may be defined in the corresponding manner. Algorithm 3.1 therefore also generalizes directly to three dimensions. In fact, it is straightforward to see that, with the exception of the proof of Lemma 3.1, all of the remaining theory in Section 3 now generalizes immediately from two to three dimensions. Hence, in order to prove that the corresponding weakly overlapping preconditioner is optimal for tetrahedral meshes in three dimensions it is sufficient to prove Lemma 3.1 for this case. Such a proof is provided in appendix A.

It should be noted that in three dimensions the number of elements in the overlap regions when using the weakly overlapping algorithm is $O(h^{-2})$ as opposed to $O(h^{-3})$ when a standard generous overlap is used. Similarly, for practical (non-optimal) two level AS algorithms with a fixed number

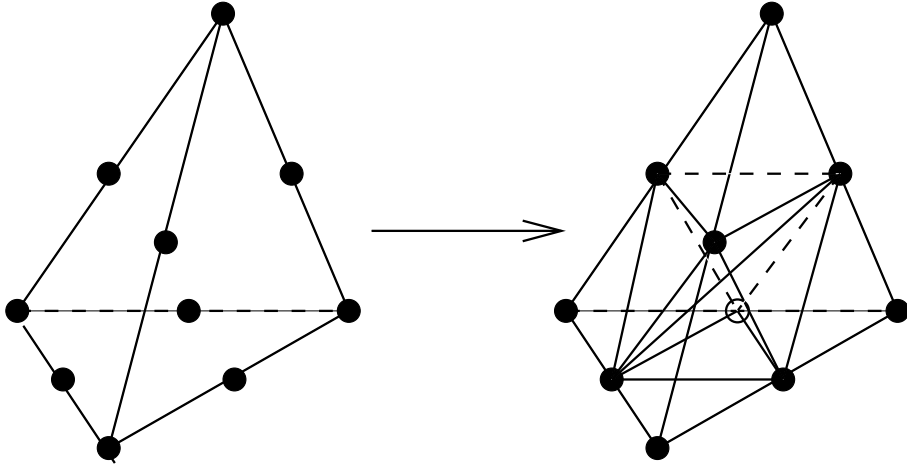


Figure 8: Refinement of a tetrahedron into 8 children by bisecting each edge.

of fine mesh layers in the overlap region, the number of elements in the overlap is also $O(h^{-2})$ in three dimensions. We again see therefore that the weakly overlapping approach has approximately the same cost (and communication overhead) per iteration as the practical small overlap two level algorithms but with the advantage of guaranteed optimality.

Having discussed the generalization of the main theoretical result of this paper to three dimensions we now illustrate this with some further numerical examples. These examples have been chosen to correspond to the two-dimensional examples already considered in the previous section.

Problem 5.1

$$\begin{aligned} -\underline{\nabla} \cdot (\underline{\nabla} u) &= f \quad \forall \underline{x} \in \Omega \equiv (0, 1) \times (0, 1) \times (0, 1), \\ u &= g \quad \forall \underline{x} \in \partial\Omega. \end{aligned}$$

Problem 5.2

$$\begin{aligned} -\underline{\nabla} \cdot \left(\begin{pmatrix} 10^2 & 0 & 0 \\ 0 & 1 & 0 \\ 0 & 0 & 1 \end{pmatrix} \underline{\nabla} u \right) &= f \quad \forall \underline{x} \in \Omega \equiv (0, 1) \times (0, 1) \times (0, 1), \\ u &= g \quad \forall \underline{x} \in \partial\Omega. \end{aligned}$$

Here f has again been chosen in each case so as to permit the exact solution $u = g$ throughout Ω .

Problem 5.3

$$\begin{aligned} -\underline{\nabla} \cdot (\underline{\nabla} u) &= f \quad \forall \underline{x} \in \Omega \equiv (0, 1) \times (0, 1) \times (0, 1), \\ u &= g \quad \forall \underline{x} \in \partial\Omega, \end{aligned}$$

where f and g are now chosen so that the analytic solution is given by:

$$u = (1 - (2x_1 - 1)^{70})(1 - (2x_2 - 1)^{70})(1 - (2x_3 - 1)^{70}) \quad \forall \underline{x} \in \Omega. \quad (5.1)$$

Table 4 presents iteration counts for Problems 5.1 and 5.2 using the weakly overlapping preconditioner on a coarse grid of 384 elements using between 1 and 4 levels of uniform mesh refinement for

Fine mesh size	Problem 5.1	Problem 5.2	Procs.
3072	7	8	2
24576	8	9	
196608	10	10	
1572864	10	11	
3072	13	13	4
24576	14	15	
196608	15	16	
1572864	16	17	
3072	13	13	8
24576	17	18	
196608	17	18	
1572864	16	17	
3072	12	13	16
24576	20	21	
196608	18	20	
1572864	17	17	

Table 4: The number of iterations required to reduce the 2-norm of the residual by a factor of 10^6 using the weakly overlapping AS preconditioner when solving Problems 5.1 and 5.2 using piecewise linear finite elements.

a typical set of partitions into 2, 4, 8 and 16 subdomains. It may be observed that the number of iterations is indeed independent of h . Furthermore, as p increases the number of iterations appears to have almost stopped growing by the time $p = 16$.

To solve Problem 5.3 local h -refinement has been used with a slightly larger coarse grid, containing 3072 tetrahedral elements. As in two dimensions the precise choice of partition of this grid is important in terms of both the final load balance and the total numbers of iterations required. Table 5 presents iteration counts for one such set of partitions into 2, 4, 8 and 16 subdomains. Again we see that the number of iterations is almost independent of h already (after just 4 levels of refinement). The partition into 16 for this problem is probably far from optimal (since simple recursive coordinate bisection, [34], was used), which may well account for the noticeable jump in iterations between $p = 8$ and $p = 16$. Nevertheless, these simple numerical experiments do show that the weakly overlapping technique can be effectively implemented in three dimensions as well as two.

Refinements (Elements/Vertices)	$p = 2$	$p = 4$	$p = 8$	$p = 16$
1 (20832/4403)	11	15	19	25
2 (198816/22237)	14	17	20	27
3 (499123/100708)	15	18	21	28
4 (2139159/429435)	17	21	24	30

Table 5: The number of iterations required to reduce the 2-norm of the residual by a factor of 10^6 using the weakly overlapping AS preconditioner when solving Problem 5.3 using piecewise linear finite elements.

6 Discussion

In this paper we have presented a two level additive Schwarz preconditioner based upon a weakly overlapping domain decomposition of a nested sequence of meshes, $\mathcal{T}_0, \dots, \mathcal{T}_J$. Such a decomposition involves just a single element of overlap at each level of the mesh hierarchy and so requires only $O(h^{-1})$ overlapping elements in total in two dimensions (and $O(h^{-2})$ in three dimensions). It has been demonstrated that, when combined with the full coarse mesh space \mathcal{W}_0 , the splitting that is induced by this decomposition is stable and therefore leads to an optimal preconditioner. Although the work presented here is for an additive Schwarz algorithm there is no reason why the same splitting should not also be used in a multiplicative manner. The resulting preconditioner will again be optimal. The extension of this approach to a multilevel algorithm is less interesting however since this leads to a standard multilevel Schwarz scheme (see [30] for example), with subdomains chosen to be the same at each level and with the overlap chosen to be minimal at each level. Such schemes are already known to be optimal.

Although the paper concentrates mainly on test problems of the form (1.1) – (1.3) in two dimensions, all aspects of the theory in Sections 2 and 3 is extended to three-dimensional problems using nested tetrahedral meshes in Section 5. Supporting numerical experiments in both two and three dimensions are also provided. Furthermore, the simplifying assumption of zero Dirichlet boundary conditions throughout $\partial\Omega_E$ may also be dropped, so as to include other Dirichlet conditions or even mixed conditions, without significant modification. Further extensions may also be made within the theoretical framework described by permitting the initial mesh, \mathcal{T}_0 , to have unequal element sizes. This would therefore allow the use of a different value for H , the size of the elements of the coarse mesh, on each subdomain.

Acknowledgments

The work of REB was supported by the National Science Foundation under contract DMS-9706090, the work of PKJ was supported by a Research Grant from the Leverhulme Trust (whilst visiting UCSD) and by a British Council ARC grant (whilst visiting TU Chemnitz), the work of SAN was supported by the Pakistan Government (Quaid-e-Azam scholarship), and the work of SVN was supported by the Deutsche Forschungsgemeinschaft, Sonderforschungsbereich 393.

A Proof of Lemma 3.1 in Three-Dimensional Case

First we introduce the following change of variables:

$$x = H r, \quad y = H s, \quad z = H t; \quad (x, y, z) \in \Omega_i. \quad (\text{A.1})$$

Under this transformation the domain Ω_i is the image of a domain Ω'_i whose geometric properties are independent of H in the (r, s, t) plane. Furthermore

$$\frac{1}{H^2} \|w_i^h(x, y, z)\|_{\mathcal{L}^2(\Omega_i)}^2 + |w_i^h(x, y, z)|_{\mathcal{H}^1(\Omega_i)}^2 = H \left(\|w_i^h(r, s, t)\|_{\mathcal{L}^2(\Omega'_i)}^2 + |w_i^h(r, s, t)|_{\mathcal{H}^1(\Omega'_i)}^2 \right), \quad (\text{A.2})$$

and we may define by $Q'_{i,k}$ the projection in the (r, s, t) variables which corresponds to $Q_{i,k}$. From [9] and [26] it follows that there exists $C_2 > 0$, which is independent of h, H and p , such that:

$$\frac{1}{H^2} \sum_{k=0}^J 4^k \|v_{i,k}^h\|_{\mathcal{L}^2(\Omega_i)}^2 = \frac{1}{H^2} \left(\|Q_{i,0} w_i^h(x, y, z)\|_{\mathcal{L}^2(\Omega_i)}^2 + \sum_{k=1}^J 4^k \|(Q_{i,k} - Q_{i,k-1}) w_i^h(x, y, z)\|_{\mathcal{L}^2(\Omega_i)}^2 \right)$$

$$\begin{aligned}
&= H \left(\|Q'_{i,0} w_i^h(r, s, t)\|_{\mathcal{L}^2(\Omega'_i)}^2 + \sum_{k=1}^J 4^k \|(Q'_{i,k} - Q'_{i,k-1}) w_i^h(r, s, t)\|_{\mathcal{L}^2(\Omega'_i)}^2 \right) \\
&\leq HC_2 \|w_i^h(r, s, t)\|_{\mathcal{H}^1(\Omega'_i)}^2 \\
&= C_2 \left(\frac{1}{H^2} \|w_i^h(x, y, z)\|_{\mathcal{L}^2(\Omega_i)}^2 + |w_i^h(x, y, z)|_{\mathcal{H}^1(\Omega_i)}^2 \right). \tag{A.3}
\end{aligned}$$

A second inequality that we require comes from [26], where it is shown that there exists $C_3 > 0$, which is independent of h , H and p , such that

$$\begin{aligned}
\|\hat{v}_i^h(x, y, z)\|_{\mathcal{H}^1(\hat{\Omega}_i)}^2 &= H^3 \|\hat{v}_i^h(r, s, t)\|_{\mathcal{L}^2(\hat{\Omega}'_i)}^2 + H |\hat{v}_i^h(r, s, t)|_{\mathcal{H}^1(\hat{\Omega}'_i)}^2 \\
&\leq HC_3 \inf_{\substack{\hat{v}_i^h = \hat{\xi}_0 + \dots + \hat{\xi}_J \\ (\hat{\xi}_k \in \hat{\mathcal{W}}'_{i,k})}} \sum_{k=0}^J 4^k \|\hat{\xi}_k\|_{\mathcal{L}^2(\hat{\Omega}'_i)}^2, \tag{A.4}
\end{aligned}$$

where $\hat{\mathcal{W}}'_{i,k}$ is the space which corresponds to $\hat{\mathcal{W}}_{i,k}$ with the change of variables (3.28). From this, along with (3.25) and (A.3), it follows that

$$\begin{aligned}
\|\hat{v}_i^h(x, y, z)\|_{\mathcal{H}^1(\hat{\Omega}_i)}^2 &\leq HC_3 \sum_{k=0}^J 4^k \|\hat{v}_{i,k}^h\|_{\mathcal{L}^2(\hat{\Omega}'_i)}^2 \\
&= \frac{C_3}{H^2} \sum_{k=0}^J 4^k \|\hat{v}_{i,k}^h\|_{\mathcal{L}^2(\hat{\Omega}_{i,k})}^2 \\
&\leq \frac{C_0 C_3}{H^2} \sum_{k=0}^J 4^k \|v_{i,k}^h\|_{\mathcal{L}^2(\Omega_i)}^2 \\
&\leq C_0 C_2 C_3 \left(\frac{1}{H^2} \|w_i^h\|_{\mathcal{L}^2(\Omega_i)}^2 + |w_i^h|_{\mathcal{H}^1(\Omega_i)}^2 \right). \tag{A.5}
\end{aligned}$$

as required. ///

References

- [1] M. Ainsworth and J.T. Oden, “*A Posterior Error Estimation in Finite Element Analysis*”, Wiley, Chichester, 2000.
- [2] S.F. Ashby, T.A. Manteuffel and P.E. Taylor, “*A Taxonomy for Conjugate Gradient Methods*”, SIAM J. on Numerical Analysis, 27, 1542–1568, 1990.
- [3] R.E. Bank, T. Dupont and H. Yserentant, “*The Hierarchical Basis Multigrid Method*”, Numerische Mathematik, 52, 427–458, 1988.
- [4] R.E. Bank and M. Holst, “*A New Paradigm for Parallel Adaptive Meshing Algorithms*”, SIAM J. on Scientific Computing, 22, 1411–1443, 2000.
- [5] R.E. Bank and P.K. Jimack, “*A New Parallel Domain Decomposition Method for the Adaptive Finite Element Solution of Elliptic Partial Differential Equations*”, Concurrency and Computation: Practice and Experience, 13, 327–350, 2001.

- [6] R.E. Bank and R.K. Smith, “*The Incomplete Factorization Multigraph Algorithm*”, SIAM J. on Scientific Computing, 20, 1349-1364, 1999.
- [7] R.E. Bank and C. Wagner, “*Multilevel ILU Decomposition*”, Numerische Mathematik, 82, 543-576, 1999.
- [8] R.E. Bank and J. Xu, “*A Hierarchical Basis Multigrid Method for Unstructured Meshes*”, in Tenth GAMM-Seminar Kiel on Fast Solvers for Flow Problems (W. Hackbusch and G. Wittum, eds.), Vieweg-Verlag, Braunschweig, 1995.
- [9] V. Bornemann and H. Yserentant, “*A Basic Norm Equivalence for the Theory of Multilevel Methods*”, Numerische Mathematik, 64, 455–476, 1993.
- [10] J. Bramble, J. Pasciak and J. Xu, “*Parallel Multilevel Preconditioners*”, Mathematics of Computation, 55, 1–21, 1990.
- [11] T. Chan and T. Matthew, “*Domain Decomposition Algorithms*”, Acta Numerica, 61–143, 1994.
- [12] T. Chan, B. Smith, and J. Zou, “*Overlapping Schwarz Methods on Unstructured Meshes using Non-matching Coarse Grids*”, Numerische Mathematik, 73, 149–167, 1995
- [13] M. Dryja and O.B. Widlund, “*Towards a Unified Theory of Domain Decomposition Algorithms for Elliptic Problems*”, in Third International Symposium on Domain Decomposition Methods (T.F. Chan *et al.*, eds.), SIAM publications, Philadelphia, 1990.
- [14] M. Dryja and O.B. Widlund, “*Some Domain Decomposition Algorithms for Elliptic Problems*”, in Iterative Methods for Large Linear Systems, Academic Press, 1990.
- [15] M. Dryja and O.B. Widlund, “*Multilevel Additive Methods for Elliptic Finite Element Problems*”, in Proceedings of sixth GAMM-seminar (W. Hackbusch ed.), Vieweg, Braunschweig, Germany, 1991.
- [16] C. Farhat, J. Mandel and F.X. Roux, “*Optimal Convergence Properties of the FETI Domain Decomposition Method*”, Computer Methods for Applied Mechanics and Engineering, 115, 365–385, 1994.
- [17] G.H. Golub and C.F. Van Loan, “*Matrix Computations*”, John Hopkins Press, 3rd edition, 1996.
- [18] M. Griebel and P. Oswald, “*On Additive Schwarz Preconditioners for Sparse Grid Discretizations*”, Numerische Mathematik, 66, 449–463, 1994.
- [19] G. Haase, U. Langer, A. Meyer and S.V. Nepomnyaschikh, “*Hierarchical Extension Operators and Local Multigrid Methods in Domain Decomposition Preconditioners*”, East-West J. Numer. Math., 2, 172–193, 1994.
- [20] G. Haase and S.V. Nepomnyaschikh, “*Explicit Extension Operators on Hierarchical Grids*”, East-West J. Numer. Math., 5, 231–248, 1997.
- [21] M.E. Hayder, D.E. Keyes and P. Mehrotra, “*A Comparison of PETSc Library and HPF Implementations of an Archetypal PDE Computation*”, Advances in Engineering Software, 29, 415-424, 1998.

- [22] D.C. Hodgson and P.K. Jimack, “*A Domain Decomposition Preconditioner for a Parallel Finite Element Solver on Distributed Unstructured Grids*”, *Parallel Computing*, 23, 1157–1181, 1997.
- [23] C. Johnson “*Numerical Solution of Partial Differential Equations by the Finite Element Method*”, Cambridge University Press, 1987.
- [24] P. LeTallec, “*Domain Decomposition Methods in Computational Mechanics*”, *Comput. Mech. Adv.*, 2, 121–220, 1994.
- [25] A.M. Matsokin and S.V. Nepomnyaschikh, “*Schwarz Alternating Method in Subspaces*”, *Soviet Mathematics*, 29, 78–84, 1985.
- [26] P. Oswald, “*Multilevel Finite Element Approximation: Theory and Applications*”, B.G. Teubner, Struttgart, 1994.
- [27] A. Quarteroni and A. Valli, “*Domain Decomposition Methods for Partial Differential Equations*”, Clarendon Press, Oxford; New York, 1999.
- [28] W. Rachowicz, “*An Overlapping Domain Decomposition Preconditioner for an Anisotropic h-Adaptive Finite Element Method*”, *Computer Methods for Applied Mechanics and Engineering*, 127, 269–292, 1995.
- [29] M.-C. Rivara, “*A Grid Generator Based on 4-Triangles Conforming Mesh Refinement Algorithm*”, *Int. J. Numer. Meth. Eng.*, 24, 1343–1354, 1987.
- [30] B. Smith, P. Bjorstad and W. Gropp, “*Domain Decomposition: Parallel Multilevel Methods for Elliptic Partial Differential Equations*”, Cambridge University Press, 1996.
- [31] W. Speares and M. Berzins, “*A 3-d Unstructured Mesh Adaptation Algorithm for Time-Dependent Shock Dominated Problems*”, *International Journal for Numerical Methods in Fluids*, 25, 81–104, 1997.
- [32] N. Touheed, P. Selwood, P.K. Jimack and M. Berzins, “*A Comparison of Some Dynamic Load-Balancing Algorithms for a Parallel Adaptive Flow Solver*”, *Parallel Computing*, 26, 1535–1554, 2000.
- [33] O.B. Widlund, “*Some Schwarz Methods for Symmetric and Nonsymmetric Elliptic Problems*”, in *Fifth International Symposium on Domain Decomposition Methods* (D.E. Keyes *et al*, eds.), SIAM publications, Philadelphia, 1992.
- [34] R.D. Williams, “*Performance of Dynamic Load Balancing for Unstructured Mesh Calculations*”, *Concurrency: Practice and Experience*, 3, 457–481, 1991.
- [35] R. Verfürth, “*A review of A Posteriori Error Estimation and Adaptive Mesh Refinement Techniques*”, Wiley-Teubner, Chichester; Stuttgart, 1996.
- [36] J. Xu, “*Iterative Methods by Space Decomposition and Subspace Correction*”, *SIAM Review*, 34, 581–613, 1992.
- [37] J. Xu and J. Zou, “*Some Nonoverlapping Domain Decomposition Methods*”, *SIAM Review*, 40, 857–914, 1998.
- [38] X. Zhang, “*Multilevel Schwarz Methods*”, *Numerische Mathematik*, 63, 521–539, 1992.